

Ground Thermal Response to Borehole Ground Heat Exchangers

O. Mikhaylova, I.W. Johnston & G.A. Narsilio
The University of Melbourne, Melbourne, Australia

ABSTRACT: Ground heat exchangers (GHEs) are the elements of ground source heat pump (GSHP) systems that provide thermal interactions with the ground. Closed-loop borehole GHEs are commonly used for GSHP systems in urban areas where land availability can be limited. The installation costs of borehole GHEs are usually the largest component of the capital costs of GSHP systems. More research, including experimental studies, into GHEs can improve GHE design and reduce their costs. This paper presents the first findings of a full-scale experimental study of the ground thermal response to a 120 kW commercial GSHP system in Melbourne, Australia. The system uses twenty-eight 50 m deep borehole GHEs to interact with the ground. Several temperature monitoring boreholes were installed close to some of the GHEs to monitor their thermal impact on the ground. The first sets of ground monitoring data are summarised to show trends of ground thermal disturbance by real-life thermal loads.

1 INTRODUCTION

Ground heat exchangers (GHEs) are the key elements of ground source heat pump (GSHP) systems which provide thermal interactions between the ground and the fluid circulating within the systems. The installation costs of GSHP systems largely depend on the costs of GHEs, so an optimum design of GHEs is important for financial feasibility of such systems. More research, including experimental studies, should be undertaken into GHE-ground thermal interactions, so that more informative design decisions can be made in sizing of GHEs.

Yavuzturk & Spitzer (2001) summarised criteria for the experimental data sets for GHE model validations. Such observations should be continuously collected from the beginning of the system operation and include, at least, measurements of inlet and outlet circulation fluid temperatures and fluid flow rates over time. Also, such data sets should provide accurate information about the geometrical parameters of the GHEs and thermal properties of the ground, grout and circulating fluid. If obtained, such data sets can be used to extend understanding of thermal processes during GHE-ground interactions and to validate GHE analytical and numerical models.

Even though quite a few experimental studies into GSHP systems have been published, quality monitoring data sets involving relatively long-term performance of GHEs under real-life building loads are rare. In addition, there have been only a few experi-

mental studies of the thermal response of the ground around GHEs. Recently, Cullin et al. (2015) commented that the observational data of the quality that is suitable for the validation of GHE design methodologies is difficult to obtain.

The Elizabeth Blackburn School of Sciences (EBSS) full-scale shallow geothermal installation in Melbourne, Australia was designed to study ground thermal reactions to borehole GHEs. The GSHP system is heavily instrumented to monitor power and energy input and output, GHE fluid temperatures throughout the system, ground temperatures around GHEs at different depths, undisturbed ground temperatures, building thermal loads and on-site weather. The system was commissioned in March, 2014 and has been in continuous operation since.

This paper presents some of the first observations of the EBSS instrumental installation. Based on this data, a number of performance characteristics have been observed. It is suggested that these characteristics should be taken into account when developing more comprehensive design methodologies.

2 EXPERIMENTAL SET-UP

The 1,500 m² two-storey school building (Fig. 1) was fitted with a 120 kW GSHP system which provides heating and cooling energy. The heat pumps are coupled with twenty-eight 50 m deep double U-loop borehole GHEs (Fig. 2). Sixteen of the twenty-eight GHEs are located under the thermally insulated concrete floor slab of the building and the remaining twelve GHEs are located outside the building footprint. A view of a GHE being installed at the site is shown in Figure 3.



Figure 1. The Elizabeth Blackburn School of Sciences.

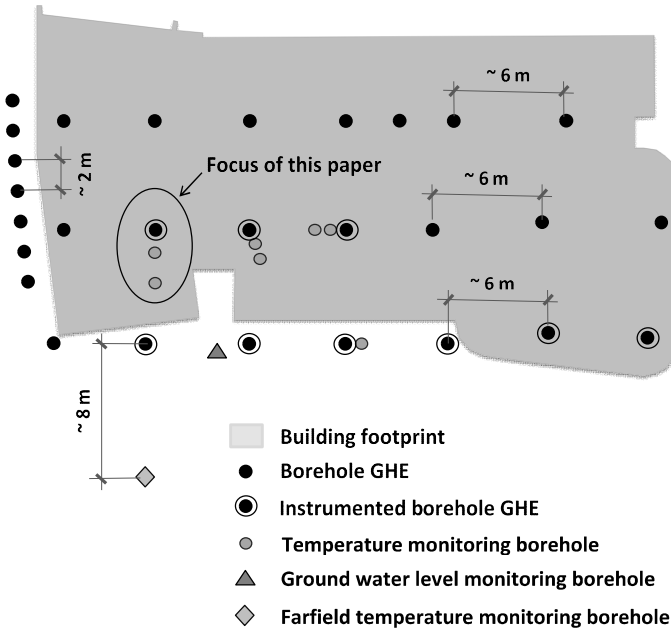


Figure 2. Location of GHEs and monitoring boreholes.

This paper focuses on the observations of grout and ground temperatures around a single GHE located under the building as indicated in Figure 2. Two ground temperature monitoring boreholes were installed to record ground temperatures around this GHE at $R = 1.3$ m and $R = 3.2$ m from its centre. A plan view section of this GHE and nearby temperature monitoring boreholes is shown in Figure 4.

The vertical location of the temperature sensors attached to the external wall of the downward (or inlet) U-loop leg of the GHE and installed in the two

monitoring boreholes is shown in Figure 5. The GHE has eleven temperature sensors installed along its downward U-loop leg. The monitoring boreholes are fitted with eleven and ten temperature sensors installed along their lengths. In addition to the grout and ground temperature sensors, inlet and outlet in-water temperature ports as well as a water flow meter were fitted into the header pipes leading to the GHE to record thermal loads applied to it.



Figure 3. A GHE being installed.

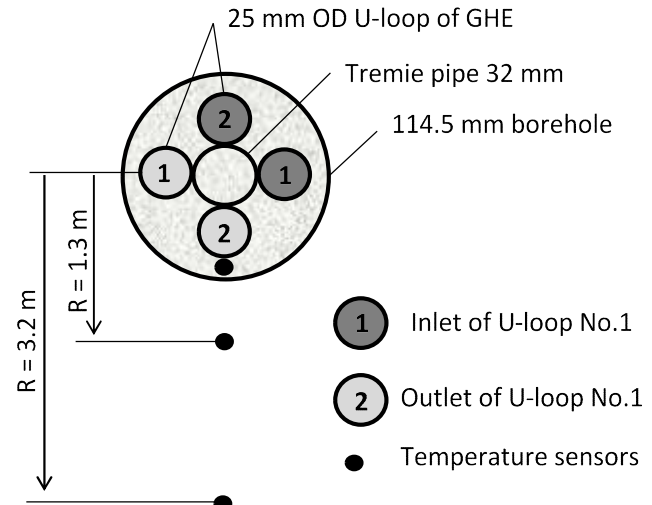


Figure 4. A plan view section of the GHE under consideration showing location of temperature sensors (not to scale).

Continuous core samples were collected from the site to study the thermal conductivity of the ground. The ground at the site from around 1.5 m and down to 50 m is Silurian mudstone (Johnston 1992). In addition, several samples of the grout were collected during the grouting of the GHEs. The thermal conductivities of the ground and grout were measured in the laboratory using a TCi scanner (www.ctherm.com). The average thermal conductivity of the ground and grout materials are around 2.7 W/(m·K) and 2.2 W/(m·K) respectively. The ground water level measured in the open borehole on the site is about 18 m below the ground surface.

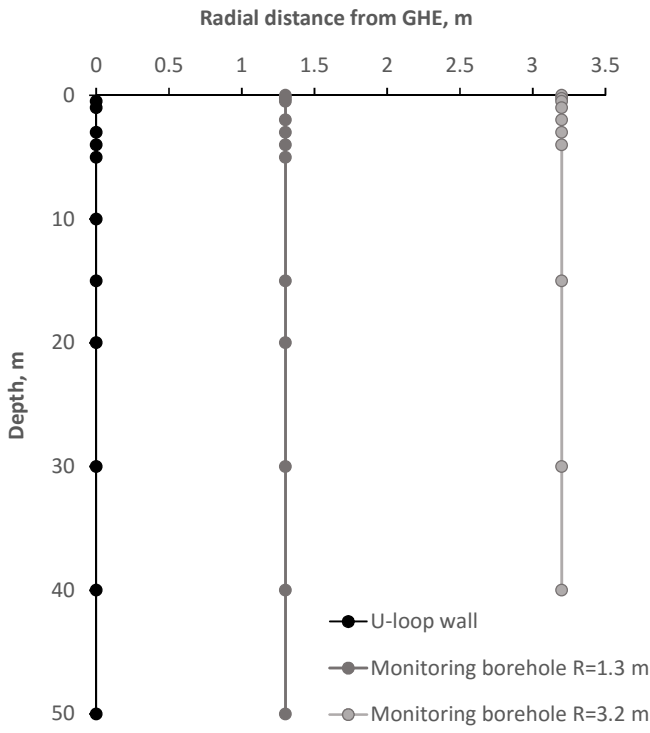


Figure 5. A vertical location of the temperature sensors attached to the outside wall of the downward U-loop leg of the GHE and installed in two monitoring boreholes. Dots indicate sensors.

3 EXPERIMENTAL OBSERVATIONS

3.1 Air and farfield ground temperatures

Figure 6 presents the outside shade air temperatures recorded on the roof of the building during a one year period starting August 2014. The maximum temperature recorded during this period was 38.6 °C in January, 2015 and the minimum temperature was 2.4 °C in July, 2015. The average air temperature during this period was 15.8 °C.

The ground temperatures at around 8 m from the installed GHEs (Fig. 2) were monitored to observe the values of the temperatures not affected by the installation or the farfield ground temperatures. Some of these observations at selected dates to a depth of about 50 m are shown in Figure 7. The ground temperatures at depths of up to 5 m were subjected to ambient temperature fluctuations whereas the temperatures below 5 m were almost constant through the year. The undisturbed ground temperature below about 5 m at the site is around 19.4 °C.

3.2 Thermal loads

The thermal loads applied to GHEs were determined by the building heating and cooling demands. Typical thermal power applied to the single monitored GHE in winter (heating) and summer (cooling) is shown in Figure 8. As seen in the figure, the GSHP system is scheduled to work from 7 am until 6 pm during weekdays and typically switched off for the

rest of the time. The heating power from the GHE normally reached around 3 kW whereas the applied cooling power to the GHE was typically a little more.

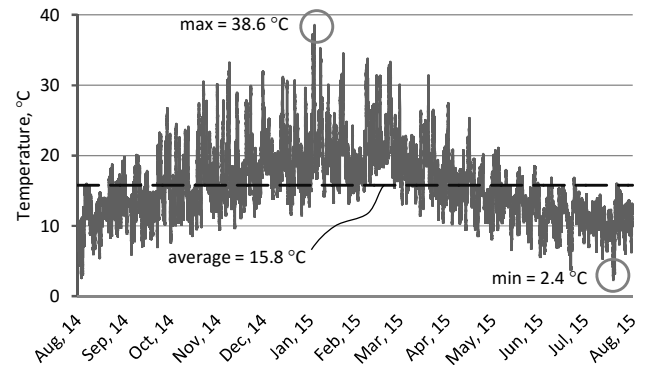


Figure 6. Annual ambient air temperatures recorded on site.

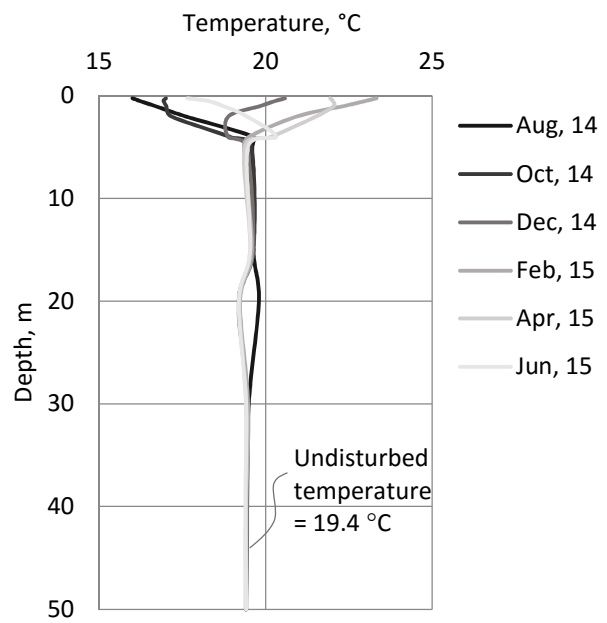


Figure 7. Farfield ground temperatures at selected dates over a year to a depth of about 50 m.

The cumulative geothermal energy to the GHE from the start of the system operation is shown in Figure 9. As observed, from approximately April to November (including a winter in Melbourne), the system mainly works in heating. From approximately November to April (including a summer in Melbourne) the system predominantly works in cooling.

When the system started operation in March, 2014, the cumulative ground energy was zero. By March, 2015, after a full year of operation, this one GHE extracted 1,336 kWh of geothermal energy for heating and injected 1,732 kWh for cooling. In total, the GHE supplied around 3,070 kWh of geothermal energy for air-conditioning the building. In March, 2015, the cumulative heating applied to the GHE reached 397 kWh (cooling). This demonstrates that the overall annual load applied to the ground throughout the first year of operation (from March,

2014 to March, 2015) was cooling dominant with a net injection of thermal load to the ground of nearly 400 kWh per GHE.

The overall maximum cumulative heating energy extracted from the GHE reached around -800 kWh. The overall maximum cumulative cooling energy applied to the GHE was slightly more than 600 kWh.

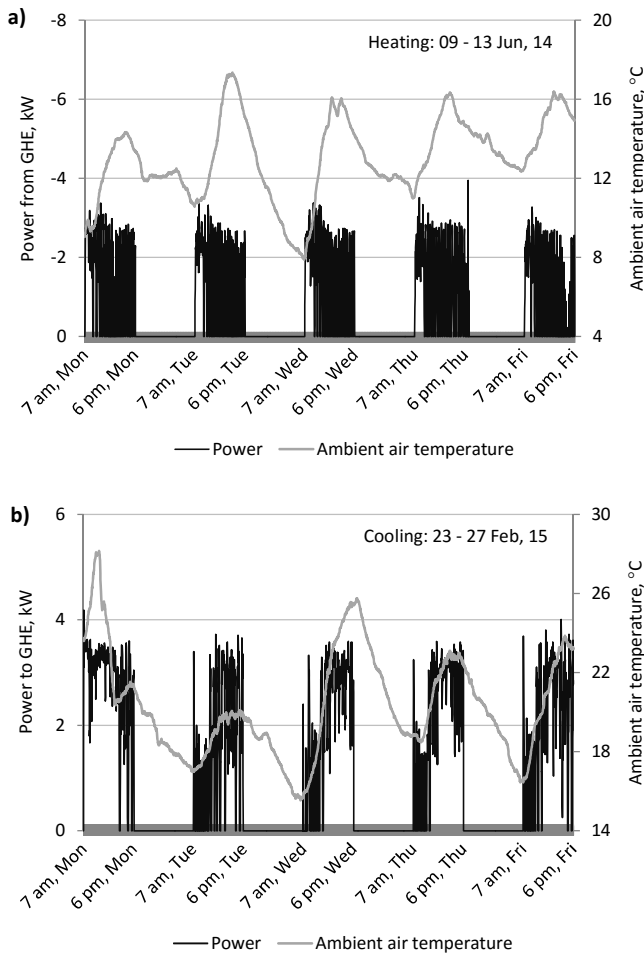


Figure 8. Typical geothermal power to the GHE during a) heating in winter and b) cooling in summer.

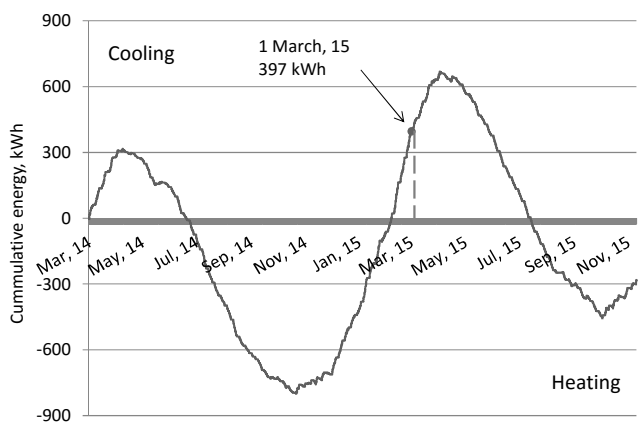


Figure 9. Cumulative ground load applied through the GHE.

3.3 Grout and ground thermal reactions to GHE

Grout and ground thermal properties, including thermal conductivity, diffusivity and temperatures, determine the performance of GHEs. Temperatures around GHEs might substantially change during operation of a system and can, therefore, affect its performance, especially in the long-term. It is important to anticipate this aspect of system operation and consider it in the design of GHEs.

In the EBSS facility, grout and ground thermal reactions to GHEs have been being studied in detail. Some observations on the grout and ground temperatures at different stages of the system operation are presented in this section of the paper.

3.3.1 Grout and ground temperatures along and around GHE

To demonstrate grout thermal response along the GHE, the observations of three sensors – at 0.5 m, 30 m and 50 m below the underside of the building slab – were selected for presentation and discussion. These sensors are attached to the outside wall of the downward U-loop leg of the GHE. The annual temperatures recorded by these sensors are shown in Figure 10.

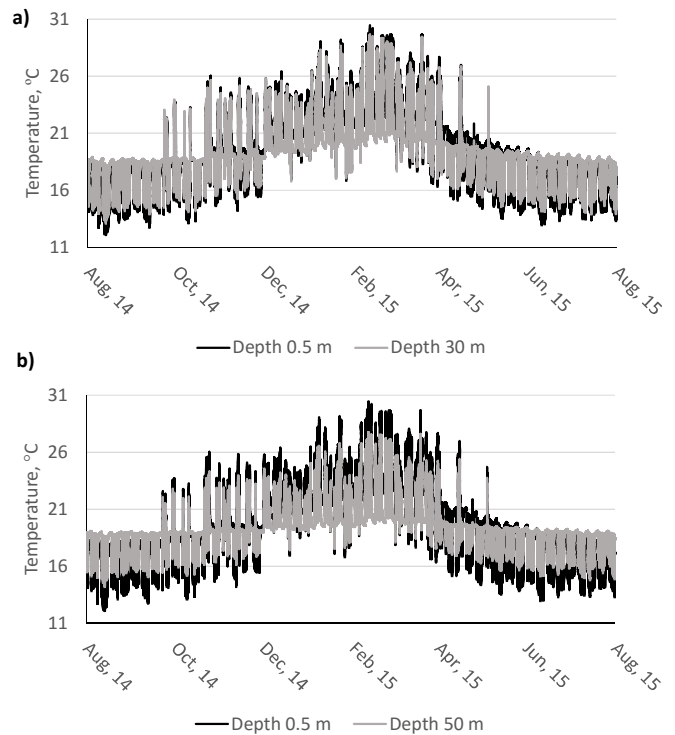


Figure 10. Annual observations of the temperatures of the outside wall of the downward U-loop leg of the GHE at a) 0.5 m and 30 m and b) 0.5 m and 50 m below the underside of the building slab.

Generally, as shown in the figure, the 0.5 m sensor recorded lower temperature peaks in heating and higher temperature peaks in cooling compared to the 30 m and 50 m sensors. Also, the observed temperature peaks at the depth of 30 m are lower in heating and higher in cooling than at a depth of 50 m. As an example, the minimum temperatures in heating at

these sensors were observed on 13 August, 2014 with 12.1 °C recorded at 0.5 m, 13.1 °C – at 30 m and 14.2 °C – at 50 m. A similar trend is observed in cooling where the maximum temperatures at these sensors were on 11 February, 2015 with 30.5 °C recorded at 0.5 m, 29.7 °C – at 30 m and 27.8 °C – at 50 m.

These observations demonstrate that the grout is affected by heat extraction or injection unevenly along the length of the GHE. In particular, the grout thermal disturbances (or its temperature deviations from the undisturbed ground temperature of 19.4 °C) in both heating and cooling were higher at the top part of the GHE and decrease with the depth of the GHE. In addition, these thermal disturbances are nonlinear along the length of the GHE. Such thermal reactions can be explained by higher heat exchange rates between the grout and circulating fluid in the top section of the GHE. Such disturbed grout temperature profile determines the pattern of the temperatures of the ground adjacent to the GHE.

To consider ground thermal disturbance around the GHE, Figure 11 shows annual changes in temperatures at 0.5 m and 30 m below the building floor slab at three radial distances from the GHE: at the downward U-loop wall, at $R = 1.3$ m and at $R = 3.2$ m. These plots demonstrate that, at both depths, for heating and cooling, the thermal disturbance is significantly higher at the U-loop wall compared to the thermal disturbance at 1.3 m and 3.2 m distances. Indeed, over the monitoring period, at the depth of 0.5 m, the maximum temperature at the U-loop wall was 30.5 °C whereas at 1.3 m and 3.2 m, the maximum temperatures were 21.8 °C and 21.3 °C respectively. At the depth of 30 m, the maximum temperature at the U-loop wall was 29.7 °C whereas at 1.3 m and 3.2 m, the maximum temperatures were 20.5 °C and 19.8 °C respectively. A similar trend is observed in heating. Overall, the ground temperatures follow a similar trend as the grout temperatures with higher cooling and lower heating peaks recorded at the 0.5 m depth compared to the 30 m depth at the same radial distances.

Figure 12 presents a vertical profile of the ground temperatures at and around the GHE at depths of up to 50 m from the underside of the building slab for the same radial locations as considered previously. For this plot, the temperatures at U-loop walls were considered at the end of night recovery (just before the GSHP system switched on at 7 am each day, see Figures 8). This excludes immediate temperature rises and drops at the U-loop wall due to the temperature of the water circulating inside the GHE. Also, after a night recovery, the temperatures at the sensors attached to the downward and upward U-legs at the same depths normally equalise. Hence, the grout temperatures at these times show general temperature trends of the grout.

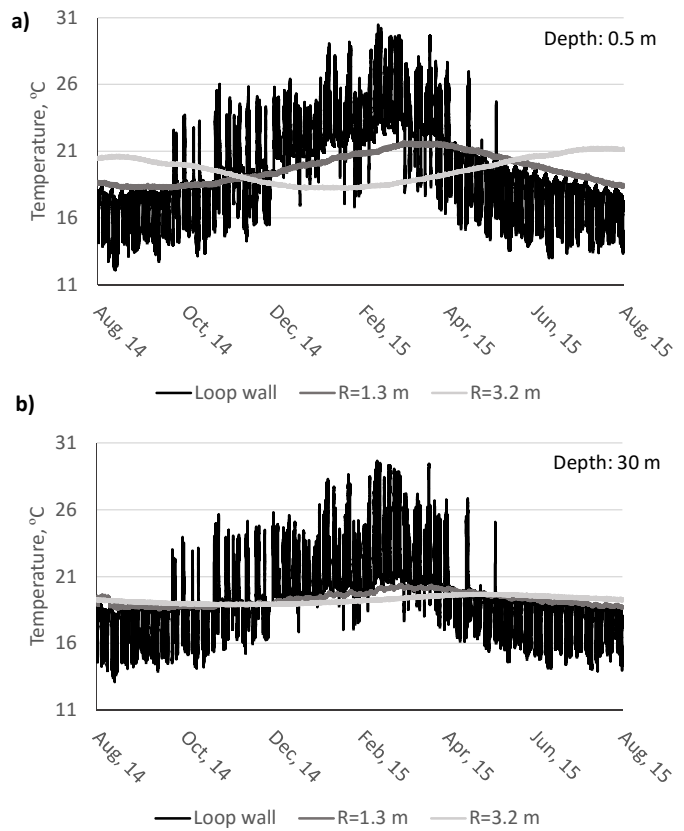


Figure 11. Annual observations of the temperatures of the ground at a) 0.5 m and b) 30 m below the underside of the building slab at the outside wall of the downward U-loop leg of the GHE at $R = 1.3$ m and $R = 3.2$ m radially from the GHE.

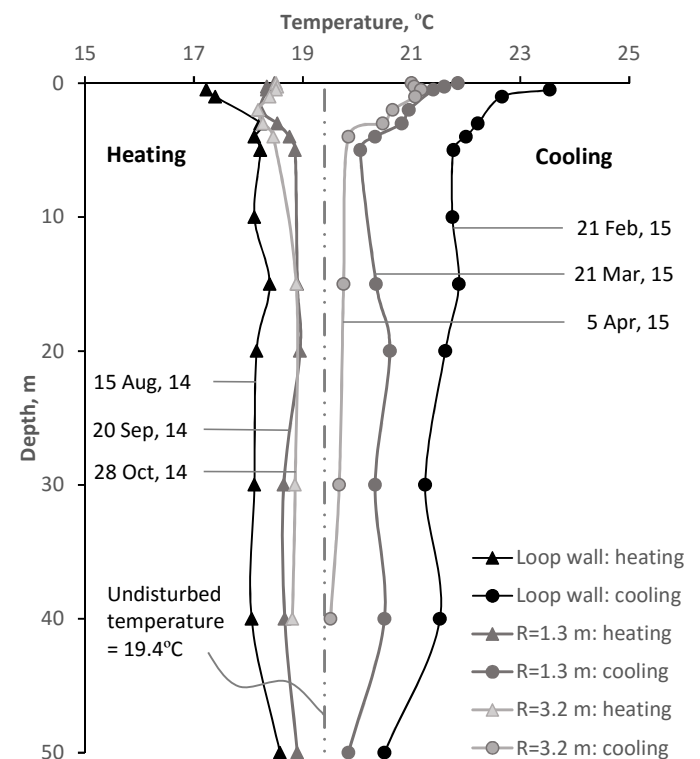


Figure 12. Minimum and maximum average temperatures along the length of the GHE for the grout and the ground at $R = 1.3$ m and $R = 3.2$ m radially from the GHE.

At different depths, the grout and ground temperatures reached peaks at different times (see, for example, Fig. 11). For Figure 12, for each radial location, the times were found when the maximum and minimum temperatures, averaged along the length of the GHE, occurred. Grout or ground temperatures have been plotted at these times to show their most thermally disturbed states at heating and cooling. The dates of these times are shown in the figure.

From the figure, the first 5 m of the grout and ground were considerably more thermally influenced by the GHE, both in heating and cooling. The temperature changes due to energy extractions and injections are nonlinear along the depth. Since the GHE is located under the insulated floor slab, there is only little temperature exchange with the surface. Such boundary conditions might contribute to the observed temperature profiles. In general, the deviation of the grout and ground temperature from the undisturbed ground temperature of 19.4 °C is larger in cooling compared to heating. This follows from the fact that the annual cumulative thermal load applied to the ground was cooling dominant (Fig. 9).

Figure 12 also illustrates the propagation of thermal disturbance through the ground over time. The maximum average temperature along the depth of the GHE was recorded on 21 February at the U-loop wall, on 21 March at 1.3 m and at 5 April at 3.2 m from the GHE centre. Hence, the maximum thermal disturbance in cooling occurred 28 days later at 1.3 m and 43 days later at 3.2 m from the GHE compared to the grout thermal disturbance at the U-loop wall. Similarly, the minimum values of the average temperatures were observed at 15 August, 20 September and 28 October at the U-loop wall, 1.3 m and 3.2 m from the GHE respectively.

Two points can be made based on the monitoring data presented in this section. Firstly, current analytical models of GHEs assume different grout and ground thermal reactions to those observed to be operating in the EBSS installation. For example, infinite and cylindrical line source models ignore both top and bottom boundary conditions of a GHE. This results in constant ground temperatures along the length of the GHE at any radial distance from it and at any particular point of time of GHE operation (Marcotte et al. 2010). Another popular analytical solution, the finite line source model, assumes that the surface is at a constant temperature equal to the undisturbed ground temperature at the site (Marcotte et al. 2010). Such an assumption leads to the ground vertical disturbed temperature profile different from the observed in the EBSS installation. A further study should be performed to understand how observed disturbed ground temperature patterns might affect GHE performance in a long-term. Also, further research is required to evaluate the accuracy of the GHE performance predictions made by current GHE analytical models.

Secondly, even though the GHE delivered a significant amount of geothermal energy (3,070 kWh during the first year, see Section 3.2), the resultant thermal disturbance of the ground around the GHE is not significant. Indeed, at $R = 3.2$ m, the maximum average ground temperature along the 50-m monitoring borehole was recorded on 5 April (Fig. 12). However, by this time, the ground temperatures just slightly exceeded the undisturbed ground temperature of 19.4 °C at depths below 5 m at that radial distance. At these depths, the difference between the disturbed and undisturbed temperatures was no more than about 0.5 °C. Although measurements cover only 1 year of the design period, this small difference may be desirable in an efficient design. In addition, the balancing of ground cooling with ground heating loads and ground thermal recovery appear to contribute to such a low thermal disturbance. Further observations and analysis should be undertaken to evaluate the ground thermal disturbance trends in the long-term.

3.3.2 Grout thermal recovery during nights and weekends

Since the building heating and cooling schedule includes significant periods when the GSHP system is turned off (Fig. 8), the EBSS facility provides an opportunity to observe grout thermal recovery during standby periods of the system. Figures 13 and 14 show typical temperatures of the grout at the outside wall of the downward U-loop leg of the GHE over a typical week of heating and a typical week of cooling respectively. The grout temperatures are presented for three depths, 0.5 m, 30 m and 50 m below the underside of the building slab. As shown, the temperatures followed the building operation schedule, so the grout was being thermally disturbed due to the applied thermal loads at 7 am to 6 pm during weekdays and recovering during weeknights and weekends.

During the week of heating (Fig. 13), the U-loop wall temperatures decreased each weekday starting from 7 am due to heat extraction from the ground. At nights between weekday operations, the temperatures increased because of the ground thermal recovery when the GSHP system was switched off. However, the recovery over weeknights was not complete and the U-loop wall temperatures were lower at 6 pm on Friday compared to the beginning of the week, at 7 am on Monday. During the weekend, the system was not in operation, so the grout recovery continued. The weekend recovery was significant and the wall temperatures at 7 am on Monday after the weekend were almost the same as at 7 am of the previous Monday. A similar thermal recovery trend can be observed in Figure 14 where the U-loop wall temperatures during a week of cooling are presented.

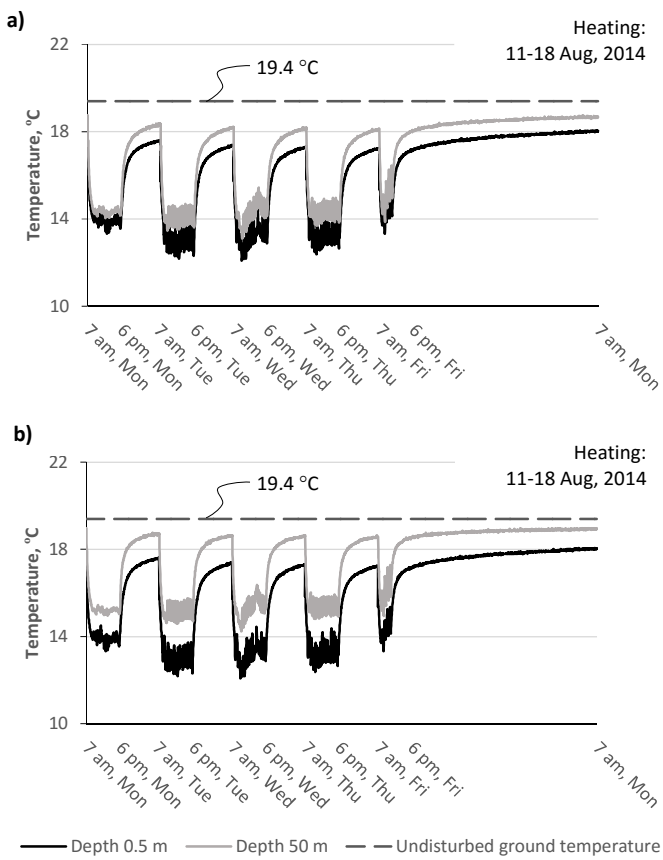


Figure 13. Typical grout temperatures at the outside wall of the downward U-loop leg of the GHE over a week of heating at a) 0.5 m and b) 30 m depths.

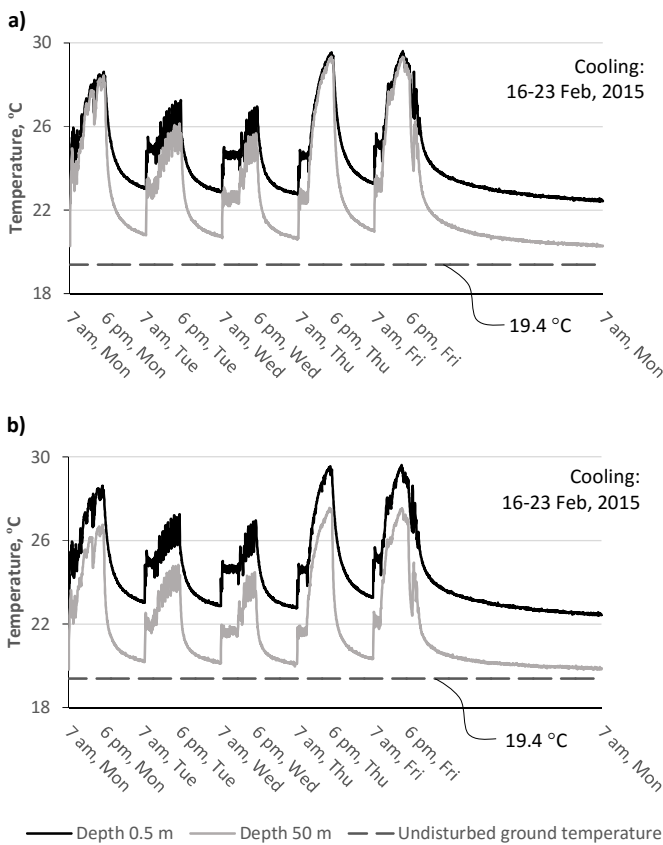


Figure 14. Typical grout temperatures at the outside wall of the downward U-loop leg of the GHE over a week of cooling at a) 0.5 m and b) 50 m depths.

Also, Figures 13 and 14 illustrate the same point made before that the grout and ground around the GHE were more thermally influenced at the top sections, closer to the slab, and the thermal disturbance decreases with depth. This can be observed by comparing the grout temperatures at three different depths plotted.

The observed trends suggest that, when the GSHP system is switched off, grout recovery occurs. The recovery over nights and especially over weekends was significant, so it can considerably influence the grout temperature around GHEs. Since the grout and ground temperatures around GHEs determine the performance of GSHP systems, grout thermal recovery can influence the design of GHEs, and particularly the required lengths of GHEs. Hence, anticipated breaks in building thermal loads, which might help to keep ground and grout temperatures within targeted operational values, should be considered in the design of GHEs.

4 CONCLUSIONS

The paper presents an overview of the first observations of the Elizabeth Blackburn School of Sciences (EBSS) full-scale shallow geothermal installation in Melbourne, Australia. The GSHP system is heavily instrumented to monitor power and energy input and output, GHE fluid temperatures throughout the system, ground temperatures around GHEs at different depths, undisturbed ground temperatures, building thermal loads and on-site weather.

The average annual ambient temperature at the site over the monitoring period was 15.8 °C. The far-field ground temperatures over the top 5 m fluctuated following the seasonal fluctuations of the ambient air temperature. The undisturbed ground temperatures at depths of 5 to 50 m were nearly constant at 19.4 °C.

During the first year of operation, a single GHE provided around 3,070 kWh of geothermal energy to heat and cool the building. Over this time, the building cooling demand was higher than its heating demand, so the annual thermal energy applied to the ground was cooling dominant with about 400 kWh more energy injected into the ground than extracted for this one GHE.

The experimental results suggest that the grout and ground thermal disturbance is nonlinear along the length of a GHE in both heating and cooling. Over the upper 5 m of the GHE, the grout and ground temperatures around the GHE were significantly lower during heating and significantly higher during cooling of the building compared to the sections below. In general, the grout and ground thermal disturbance around the GHE decreases with its depth. Existing analytical models of GHEs do not consider such disturbed ground temperature profiles

around GHEs. Further investigations are required to evaluate whether such a disturbed ground temperature pattern can significantly influence the performance of GHEs, especially in the long term, and should be considered in sizing GHEs.

When the GSHP system was in a standby mode, the grout showed significant thermal recovery. Such recovery periods seem to significantly reduce ground thermal disturbances. Hence, scheduled pauses in the building thermal loads should be anticipated and considered in the sizing of GHEs. Potentially, this can reduce design lengths of GHEs. Further research should be undertaken to investigate whether the existing GHE modelling methodologies accurately simulate ground thermal recovery when GSHP systems are switched off.

5 ACKNOWLEDGEMENT

The authors would like to acknowledge the support provided by the Sustainable Energy Pilot Demonstration (SEPD) Program funded by the Department of Economic Development, Jobs, Transport and Resources of the Government of Victoria.

6 REFERENCES

- Cullin JR, Spitler JD, Montagud C, Ruiz-Calvo F, Rees SJ, Naicker SS, Konečný P and Southard LE (2015) Validation of vertical ground heat exchanger design methodologies. *Science and Technology for the Built Environment*, Taylor & Francis, **21**(2), 137–149.
- Johnston IW (1992) Silurian and Lower Devonian engineering properties. *Engineering Geology of Melbourne*, Peck, W.A. et al (Eds), Balkema, Rotterdam.
- Marcotte D, Pasquier P, Sheriff F and Bernier M (2010) The importance of axial effects for borehole design of geothermal heat-pump systems. *Renewable Energy*, **35**(4), 763–770.
- Yavuzturk C and Spitler JD (2001) Field Validation of a Short Time Step Model for Vertical Ground-Loop Heat Exchangers. *ASHRAE Transactions*, **107**(1), 1–9.